HAL
open science

# Polarized spectroscopy and SESAM mode-locking of Tm,Ho:CALGO

Yicheng Wang, Pavel Loiko, Yongguang Zhao, Zhongben Pan, Weidong Chen, Mark Mero, Xiaodong Xu, Jun Xu, Xavier Mateos, Arkady Major, et al.

## To cite this version:

Yicheng Wang, Pavel Loiko, Yongguang Zhao, Zhongben Pan, Weidong Chen, et al.. Polarized spectroscopy and SESAM mode-locking of Tm,Ho:CALGO. Optics Express, 2022, 30 (5), pp.7883. 10.1364/OE.449626 . hal-03858695

**HAL Id: hal-03858695**

**https://hal.science/hal-03858695**

Submitted on 17 Nov 2022

**HAL** is a multi-disciplinary open access archive for the deposit and dissemination of scientific research documents, whether they are published or not. The documents may come from teaching and research institutions in France or abroad, or from public or private research centers.

L'archive ouverte pluridisciplinaire **HAL**, est destinée au dépôt et à la diffusion de documents scientifiques de niveau recherche, publiés ou non, émanant des établissements d'enseignement et de recherche français ou étrangers, des laboratoires publics ou privés.

Research Article | Vol. 30, No. 5 / 28 Feb 2022 / Optics Express 7883

Optics EXPRESS

# Polarized spectroscopy and SESAM mode-locking of Tm,Ho:CALGO

YICHENG WANG,[1] PAVEL LOIKO,[2] YONGGUANG ZHAO,[1] ZHONGBEN PAN,[1] WEIDONG CHEN,[1] MARK MERO,[1] XIAODONG XU,[3] JUN XU,[4] XAVIER MATEOS,[5,6] ARKADY MAJOR,[7] MIRCEA GUINA,[8] VALENTIN PETROV,[1] AND UWE GRIEBNER[1,*]

[1] *Max Born Institute for Nonlinear Optics and Short Pulse Spectroscopy, Max-Born-Str. 2a, 12489 Berlin, Germany*
[2] *Centre de Recherché sur les Ions, les Matériaux et la Photonique (CIMAP), UMR 6252 CEA-CNRS-ENSICAEN, Université de Caen, 6 Boulevard Maréchal Juin, 14050 Caen Cedex 4, France*
[3] *Jiangsu Key Laboratory of Advanced Laser Materials and Devices, Jiangsu Normal University, 221116 Xuzhou, China*
[4] *School of Physics Science and Engineering, Institute for Advanced Study, Tongji University, 200092 Shanghai, China*
[5] *Universitat Rovira i Virgili, Physics and Cristal·lography of Materials and Nanomaterials, FiCMA-FiCNA, Marcel·lí Domingo, 1, 43007 Tarragona, China*
[6] *Serra Húnter Fellow, Spain*
[7] *University of Manitoba, 75A Chancellors Circle, Winnipeg, MB, R3 T 5V6, Canada*
[8] *Optoelectronics Research Centre, Tampere University of Technology, PO Box 692, 33101 Tampere, Finland*
[*] *griebner@mbi-berlin.de*

**Abstract:** A Tm,Ho:CALGO laser passively mode-locked by a GaSb-based SESAM generated pulses as short as 52 fs at a central wavelength of 2015 nm with a broad spectral bandwidth of 82 nm (full width at half maximum) owing to the combined gain profiles of both dopants for σ-polarized light. The average output power reached 376 mW at a repetition rate of 85.65 MHz. In the continuous-wave regime, the laser was power scaled up to 1.01 W at 2080.6 nm with a slope efficiency of 32.0%, a laser threshold of 155 mW and π-polarized emission. Polarized spectroscopic properties of $Ho^{3+}$ ions in singly doped and codoped CALGO crystals were revisited to explain the observed laser performance.

© 2022 Optica Publishing Group under the terms of the Optica Open Access Publishing Agreement

## 1. Introduction

Ultrafast lasers operating around 2 µm are of great interest for various applications, including development of amplified systems for high harmonic generation and terahertz generation which will benefit from different wavelength scaling mechanisms [1,2], and pumping of mid-infrared (3-18 µm) ultrafast optical parametric oscillators based on non-oxide nonlinear crystals [3]. Solid-state laser emission at ~2 µm is typically achieved using Thulium ($Tm^{3+}$) or Holmium ($Ho^{3+}$) ions. For the majority of singly $Tm^{3+}$-doped laser crystals, the emission owing to the $^3F_4 \rightarrow {}^3H_6$ electronic transition peaks slightly below 2 µm overlapping with the structured water vapor absorption in the atmosphere. Without purging (e.g., with nitrogen), the achievable pulse duration in mode-locked (ML) lasers is limited to a few hundred femtoseconds in this spectral region [4].

$Ho^{3+}$-ion doping can help to avoid such absorption since the emission due to the $^5I_7 \rightarrow {}^5I_8$ transition is shifted to longer wavelengths (>2 µm). A common scheme for excitation of $Ho^{3+}$ ions is the codoping of the host matrix by $Tm^{3+}$ ions acting as sensitizers [5]. It involves (i) a strong absorption by $Tm^{3+}$ ions at ~0.8 µm (the $^3H_6 \rightarrow {}^3H_4$ transition), (ii) an efficient cross-relaxation

#449626 https://doi.org/10.1364/OE.449626
Journal © 2022 Received 25 Nov 2021; revised 28 Jan 2022; accepted 3 Feb 2022; published 23 Feb 2022

Optics EXPRESS

process, $Tm_1(^3H_4) + Tm_2(^3H_6) \rightarrow Tm_1(^3F_4) + Tm_2(^3F_4)$, populating the metastable $Tm^{3+}$ state, and (iii) an energy-transfer (ET) process, $Tm(^3F_4) \rightarrow Ho(^5I_7)$ [6], see Fig. 1. Apart from easy pumping of $Tm^{3+}$,$Ho^{3+}$-codoped materials, e.g., by Ti:Sapphire lasers or AlGaAs laser diodes, they offer increased gain bandwidth owing to the spectrally overlapping emission from both ions supporting the generation of shorter pulses [7,8].

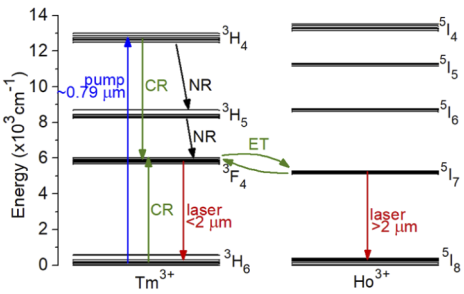


**Fig. 1.** Simplified scheme of energy-levels of $Tm^{3+}$ and $Ho^{3+}$ ions showing processes relevant for ~2 µm laser operation: CR – cross-relaxation, NR – non-radiative relaxation, ET – energy-transfer. The crystal-field splitting for CALYO can be found in [10].

Disordered host crystals are attractive for applications in femtosecond ML lasers as they provide smooth and broad emission bands of the dopant rare-earth ions. Among them, calcium rare-earth aluminates, $CaREAlO_4$ (where RE = Gd or Y, abbreviated: CALGO and CALYO, respectively), attract a lot of attention for $Tm^{3+}$ and $Ho^{3+}$ doping [9–11]. These crystals belong to the tetragonal class (space group $I_4/mmm$) exhibiting a $K_2NiF_4$ type structure and they are optically uniaxial [12]. In $CaREAlO_4$ crystals, the $Ca^{2+}$ and $RE^{3+}$ cations are statistically distributed over the same Wyckoff site (4*e*, symmetry: $C_{4v}$). The structure disorder originates from the second coordination sphere of the $RE^{3+}$ ions, i.e., a charge difference between the $Ca^{2+}$ and $RE^{3+}$ cations and a difference in the metal-to-metal distances [13]. $CaREAlO_4$ crystals exhibit a significant inhomogeneous spectral broadening of the absorption and emission bands of the dopant rare-earth ions making feasible generation of ultrashort (sub-100 fs) pulses in ML lasers [14,15]. In addition, despite their disordered nature, they feature attractive thermo-mechanical properties, i.e., high thermal conductivity with a weak dependence on the doping level, as well as nearly athermal behavior [16]. All these features determine the potential of $CaREAlO_4$ crystals for power-scalable ML lasers.

The first femtosecond ML Tm:CALGO laser was reported in 2016. Using a GaSb-based SEmiconductor Saturable Absorber Mirror (SESAM), 646 fs pulses were generated at 2021nm corresponding to an average output power of 58 mW at a pulse repetition rate of 100.6 MHz [4]. The laser was forced to oscillate above 2 µm using a dichroic mirror. Recently, we demonstrated the first sub-100-fs (87 fs) ML Tm,Ho:CALYO laser [17], in which, due to the codoping by $Ho^{3+}$ ions, the central emission wavelength was naturally shifted above 2 µm (2042.6 nm).

In the present work, we report on the polarized spectroscopy and yet shorter pulse durations from a ML Tm,Ho:CALGO laser benefiting from the combined gain bandwidth.

## 2. Polarized spectroscopy

The previously reported spectroscopic properties of $Ho^{3+}$ ions at ~2 µm in singly doped and codoped CALGO crystals are incomplete [11]. To explain properly the polarization behavior of continuous-wave (CW) and ML Tm,Ho:CALGO lasers, first, we performed a detailed polarization-resolved spectroscopic characterization. In the present work, the absorption spectra were measured using a spectrophotometer (CARY 5000, Varian). The luminescence spectra were

Optics EXPRESS

measured by an optical spectrum analyzer (model AQ6375B, Yokogawa) calibrated with a 20 W quartz iodine lamp. A Glan-Taylor prism was used for polarization-resolved studies.

A Tm,Ho:CALGO crystal grown by the Czochralski method [11] was studied. The actual (in the crystal) rare-earth doping levels were 4.5 at.% Tm and 0.5 at.% Ho. The corresponding ion densities were $N_{Tm} = 5.55\times10^{20}$ cm$^{-3}$ and $N_{Ho} = 0.62\times10^{20}$ cm$^{-3}$. The selection of concentrations of rare-earth ions for $Tm^{3+}$,$Ho^{3+}$-codoped crystals is dictated by two factors: (i) an appropriate $Ho^{3+}/Tm^{3+}$ codoping ratio, usually about 1:10 [5], suppressing the unwanted colasing of both ions in the free-running regime of operation, and (ii) a compromised $Tm^{3+}$ doping level ensuring already high enough pump absorption while still moderate energy-transfer upconversion losses.

Figure 2(a) shows the absorption band related to the $^3H_6 \rightarrow {}^3H_4$ $Tm^{3+}$ transition. The peak absorption cross-section $\sigma_{abs} = 1.53\times10^{-20}$ cm$^2$ at 792.3 nm and the absorption bandwidth (full width at half maximum, FWHM) is 17.3 nm (for π-polarization). For σ-polarized light, the absorption is much weaker, $\sigma_{abs} = 0.62\times10^{-20}$ cm$^2$ at 798.1 nm while the absorption bandwidth is similar, 17.7 nm. The broadband absorption properties of Tm,Ho:CALGO crystals facilitate their pumping by AlGaAs laser diodes emitting at ~0.79 μm. In Fig. 2(b), polarized absorption spectra around 2 μm are shown. They correspond to the spectrally overlapping $^3H_6 \rightarrow {}^3F_4$ $Tm^{3+}$ and $^5I_8 \rightarrow {}^5I_7$ $Ho^{3+}$ transitions.

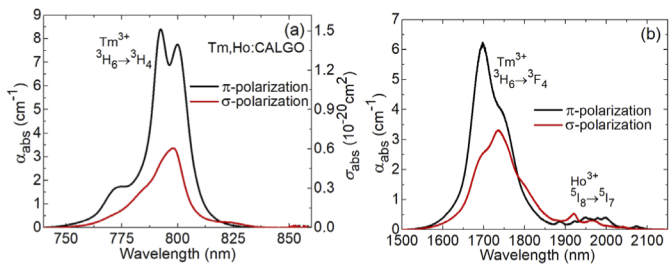


**Fig. 2.** Polarized absorption spectra of the 4.5 at.% Tm, 0.5 at.% Ho:CALGO crystal: (a) $^3H_6 \rightarrow {}^3H_4$ $Tm^{3+}$ transition, (b) $^3H_6 \rightarrow {}^3F_4$ $Tm^{3+}$ and $^5I_8 \rightarrow {}^5I_7$ $Ho^{3+}$ transitions.

Polarized luminescence spectra of the Tm,Ho:CALGO crystal are shown in Fig. 3. They are smooth and very broad spanning from 1.6 to 2.2 μm. The luminescence is due to both $^3F_4 \rightarrow {}^3H_6$ $Tm^{3+}$ and $^5I_7 \rightarrow {}^5I_8$ $Ho^{3+}$ transitions; the $Ho^{3+}$ emission dominates in the spectra. Higher emission intensity is observed for π-polarization. The spectra exhibit local peaks at 2075 and 1998 nm (π-polarization), and 2040, 1973 and 1921 nm (σ-polarization).

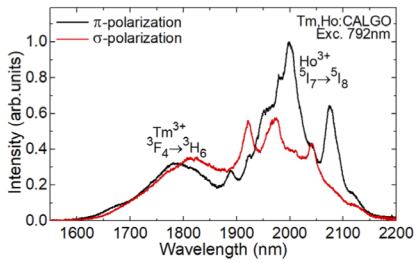


**Fig. 3.** Polarized luminescence spectra of the Tm,Ho:CALGO crystal at ~2 μm, $\lambda_{exc} = 792$ nm.

To calculate polarized gain spectra for a codoped Tm,Ho:CALGO crystal, first, we have determined the absorption, $\sigma_{abs}$, and stimulated-emission (SE), $\sigma_{SE}$, cross-section spectra for crystals singly-doped with $Tm^{3+}$ and $Ho^{3+}$ ions. Both the $^3H_6 \leftrightarrow {}^3F_4$ $Tm^{3+}$ and $^5I_8 \leftrightarrow {}^5I_7$ $Ho^{3+}$

Optics EXPRESS

transitions were considered, see Fig. 4. The discussion about the polarized emission properties of $Tm^{3+}$ ions in CALGO crystals can be found elsewhere [18]. Let us focus on the $Ho^{3+}$ ions. The SE spectra are strongly polarized. For π-polarization, the maximum $\sigma_{SE}$ is $1.05\times10^{-20}$ cm$^2$ at 1999 nm and at longer wavelengths where the laser operation is expected, another intense peak is observed ($\sigma_{SE} = 0.67\times10^{-20}$ cm$^2$ at 2075 nm). For σ-polarized light, the SE cross-sections are much lower, the maximum $\sigma_{SE}$ is $0.46\times10^{-20}$ cm$^2$ at 1972 nm and at longer wavelengths, $\sigma_{SE} = 0.40\times10^{-20}$ cm$^2$ at 2039 nm. The spectra for this polarization are less structured and strongly overlap with $Tm^{3+}$ emission. The absolute values of the SE cross-sections for $Ho^{3+}$ ions are lower than those for $Tm^{3+}$ ions due to the much longer value of the radiative lifetime of the $^5I_7(Ho^{3+})$ multiplet as compared to the $^3F_4(Tm^{3+})$ one.

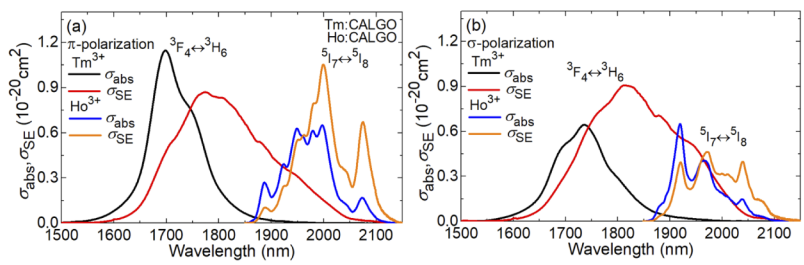


**Fig. 4.** Absorption, $\sigma_{abs}$, and stimulated-emission (SE), $\sigma_{SE}$, cross-sections for $Tm^{3+}$ and $Ho^{3+}$ ions in CALGO around ~2 μm, the light polarization is (a) π and (b) σ.

The ~2 μm transitions of both $Tm^{3+}$ and $Ho^{3+}$ ions represent a quasi-three-level laser scheme with reabsorption. Thus, gain cross-section spectra are usually calculated to conclude about the gain bandwidth, the laser wavelength and polarization:

$$\sigma_{gain,Ho} = \beta_{Ho}\sigma_{SE,Ho} - (1 - \beta_{Ho})\sigma_{abs,Ho}, \tag{1a}$$

$$\sigma_{gain,Tm} = \beta_{Tm}\sigma_{SE,Tm} - (1 - \beta_{Tm})\sigma_{abs,Tm}, \tag{1b}$$

where $\beta_{Ho} = N(^5I_7)/N_{Ho}$ and $\beta_{Tm} = N(^3F_4)/N_{Tm}$ are the inversion ratios for $Ho^{3+}$ and $Tm^{3+}$ ions, respectively. The gain profiles for $Ho^{3+}$ ions in CALGO are shown in Fig. 5(a) and 5(b). Higher gain corresponds to π-polarized light. For this polarization, the spectra are characterized by an intense and narrow peak (bandwidth: 30 nm for $\beta_{Ho} = 0.32$) whose maximum experiences a blue shift with increasing the inversion level, from 2090 nm for low $\beta_{Ho} = 0.20$ to 2075 nm for high $\beta_{Ho} = 0.44$. For σ-polarization, despite lower gain, the spectra are broader (bandwidth: 56 nm for $\beta_{Ho} = 0.32$). With increasing $\beta_{Ho}$ from 0.20 to 0.44, the maximum of the gain curves shifts from 2087 to 2042 nm. Note that when considering only $Ho^{3+}$ ions, the gain spectra extend only down to ~1975 nm.

For a codoped material, the gain spectra should be calculated accounting for the absorption and SE by both the $Tm^{3+}$ and $Ho^{3+}$ ions, as well as for the bidirectional ET between them, $Tm^{3+}(^3F_4) \leftrightarrow Ho^{3+}(^5I_7)$, establishing thermally equilibrium populations of the involved manifolds [6] and a single thermal equilibrium lifetime:

$$\sigma_{gain,eff} = \sigma_{gain,Ho}(N_{Ho}/N_{tot}) + \sigma_{gain,Tm}(N_{Tm}/N_{tot}), \tag{2}$$

where $N_{tot} = N_{Tm} + N_{Ho}$ is the total ion density and the inversion levels $\beta_{Ho}$ and $\beta_{Tm}$ are linked by the following expression [6]:

$$\beta_{Ho} = [\Omega\beta_{Tm}]/[1 + (\Omega - 1)\beta_{Tm}], \tag{3}$$

where Ω is a polarization-independent inverse equilibrium constant, corresponding to a ratio of parameters of the direct non-radiative transfer of energy ($Tm^{3+} \rightarrow Ho^{3+}$) and back ET ($Ho^{3+} \rightarrow$

Optics EXPRESS

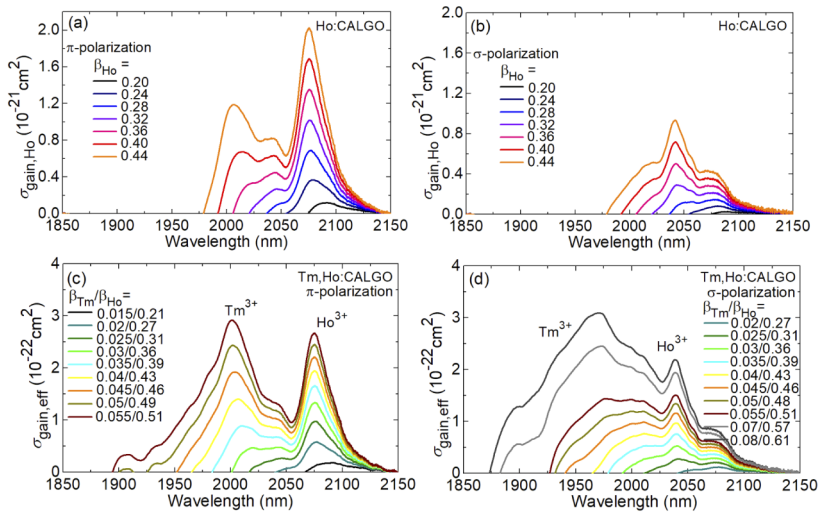


**Fig. 5.** Polarized gain spectra for the Tm,Ho:CALGO crystal at ~2 μm: (a,b) gain cross-sections for $Ho^{3+}$ ions, $\beta_{Ho} = N(^5I_7)/N_{Ho}$ is the $Ho^{3+}$ inversion ratio, (c,d) "effective" gain cross-sections accounting for the $Tm^{3+}$,$Ho^{3+}$ absorption and stimulated-emission as well as the bidirectional energy transfer between them; $\beta_{Tm} = N(^3F_4)/N_{Tm}$ is the $Tm^{3+}$ inversion ratio. The light polarizations are (a,c) π and (b,d) σ.

$Tm^{3+}$) [19]. In the present work, Ω was calculated based on the polarization-averaged, (2σ+π)/3, overlap integral between the absorption and SE spectra for $Tm^{3+}$ and $Ho^{3+}$ ions in CALGO, according to the Förster-Dexter theory [20]. The $\sigma_{gain,eff}$ values are thus calculated with respect to the total doping level ($Tm^{3+} + Ho^{3+}$). For the studied Tm,Ho:CALGO crystal, the thermal equilibrium lifetime $\tau_0$ of both the $^3F_4(Tm^{3+})$ and $^5I_7(Ho^{3+})$ multiplets is 4.3 ms.

The results on $\sigma_{gain,eff}$ for a codoped Tm,Ho:CALGO crystal are shown in Fig. 5(c,d). The spectra notably differ from those for Ho:CALGO owing to the contribution of $Tm^{3+}$ ions. For π-polarized light, the gain is higher while the spectra contain two peaks centered at 2075 and 2001nm. For the former peak, the gain bandwidth is ~30 nm ($\beta_{Tm} = 0.055$) in agreement with the value for singly $Ho^{3+}$ doping indicating no contribution from $Tm^{3+}$ ions. For σ-polarization, the spectra are smoother and much broader: for the same $\beta_{Tm} = 0.055$, the spectrum "center of gravity" is found at ~2020nm and its bandwidth is ~120 nm. Compared to Ho:CALGO, this indicates a remarkable improvement owing to the $Tm^{3+}$ contribution.

## 3. Laser performance

### 3.1. Laser set-up

For laser experiments, a rectangular sample of the same composition, 4.5 at.% Tm, 0.5 at.% Ho:CALGO, was used, cut along the ***a***-axis giving access to both π- and σ-polarizations. It had a thickness of 5.0 mm and an aperture of 4.0×4.0 $mm^2$. Both its faces were polished to laser quality and antireflection (AR) coated for the pump (~0.79 μm) and laser (~2 μm) wavelengths. The crystal was wrapped in indium foil and fixed in a copper holder providing cooling from the lateral sides. The holder was actively cooled by circulating water (16 °C).

The scheme of the laser set-up is shown in Fig. 6. An X-shaped laser cavity with two beam waists was used. The crystal was placed at normal incidence between two concave dichroic folding mirrors $M_1$ and $M_2$ (radius of curvature, RoC: -100 mm). In the short cavity arm, a curved chirped mirror ($CM_1$, RoC = -100 mm, group delay dispersion, GDD: -125 $fs^2$ per bounce) was applied to create a beam waist on a SESAM which served as an end mirror. In the long arm,

Optics EXPRESS

two plane CMs were inserted for dispersion management (GDD = -125 $fs^2$). The total round-trip GDD introduced by the CMs amounted to −1250 $fs^2$. The calculated material group velocity dispersion was -31.5 $fs^2$/mm for σ-polarization. A plane output coupler (OC) with a transmission at the laser wavelength $T_{OC} = 3.0\%$ terminated the long cavity arm. The total geometrical cavity length was 1.74 m. The calculated radii of the laser mode in the crystal and at the SESAM were 30 μm and 60 μm, respectively.

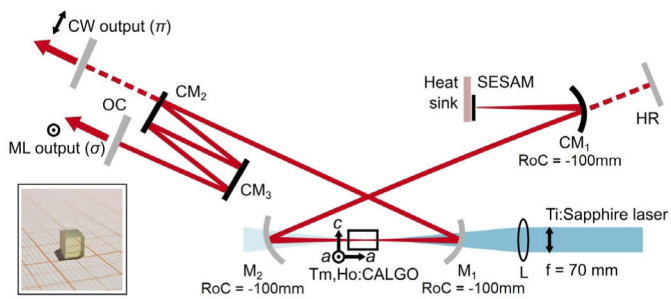


**Fig. 6.** Scheme of the ML Tm,Ho:CALGO laser: L – focusing lens, $M_1$ – curved pump mirror, $M_2$ – curved folding mirror, $CM_{1-3}$ – curved and flat chirped mirrors, OC – output coupler. *Inset* – photograph of the laser crystal.

As a pump source, we have implemented a CW Ti:Sapphire laser delivering up to 3.56 W at 791 nm (the peak absorption of $Tm^{3+}$ ions for π-polarization) with diffraction-limited beam ($M^2 \approx 1$). The pump radiation was focused into the laser crystal through the $M_1$ folding mirror using an AR-coated lens (f = 70 mm) resulting in a pump spot radius of 30 μm. The pumping was in a single pass.

As saturable absorber, we used an anti-resonant GaSb-based SESAM designed for the central wavelength of 2060 nm with two InGaAsSb quantum wells (thickness: 8.5 nm) and a 50 nm cap layer without any AR coating [21]. The recovery time of the initial absorption was measured by the pump-probe method at 2040 nm. A pulse fluence of ~50 μJ/$cm^2$ was realized with a pulse duration of 180 fs. The recorded trace and the biexponential fit to the data are shown in Fig. 7(a) revealing the intraband and interband relaxation times of $\tau_{fast} = 0.3$ ps and $\tau_{slow} = 20$ ps, respectively. Furthermore, we computed the GDD of the SESAM layer structure on the basis of its measured and designed reflectivity, Fig. 7(b). As can be seen, there is some difference between the original design and the measured reflectivity: the AlAsSb/GaSb distributed Bragg reflector gives the impression of being slightly shifted and narrower relative to the design. This difference indicates a deviation of the refractive index data in the grown structure compared to design data.

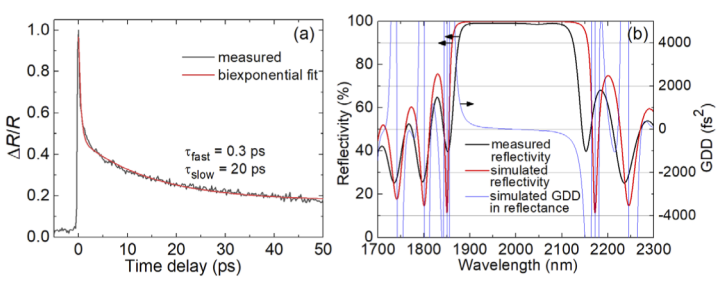


**Fig. 7.** Characterization of GaSb-based SESAM: (a) pump-probe trace at 2040 nm: experimental data (*grey*) and their biexponential fit (*red*); (b) measured (*black*) and calculated (*red*) reflectivity and calculated GDD (*blue*).

Optics EXPRESS

The designed GDD of the SESAM is also shown in Fig. 7(b). Here a GDD of < -20 $fs^2$ is deduced for the expected spectral emission of the Tm,Ho:CALGO laser, i.e., an almost zero GDD around 2000 nm. Measurement data of the modulation depth of the SESAM are not yet available. However, low non-saturable loss is confirmed by the high linear reflectivity ranging around 1%. Furthermore, a peak absorption of the two QW structure of 1.5% is deduced at 2060 nm.

### 3.2. Continuous-wave laser

First, CW laser performance of Tm,Ho:CALGO was studied by removing the flat CMs from the cavity and replacing the SESAM by a flat highly reflective (HR) mirror. Different OCs with $T_{OC}$ ranging from 0.2% to 3.0% were tested. The laser generated a maximum output power of 1.01 W at 2080.6 nm with a slope efficiency $\eta$ of 32.0% (with respect to the absorbed pump power) and a laser threshold of 155 mW (for $T_{OC}$ = 1.5%), see Fig. 8(a). The maximum optical-to-optical efficiency $\eta_{opt}$ amounted to 28.4% (vs. the incident pump power). The input-output dependences were linear.

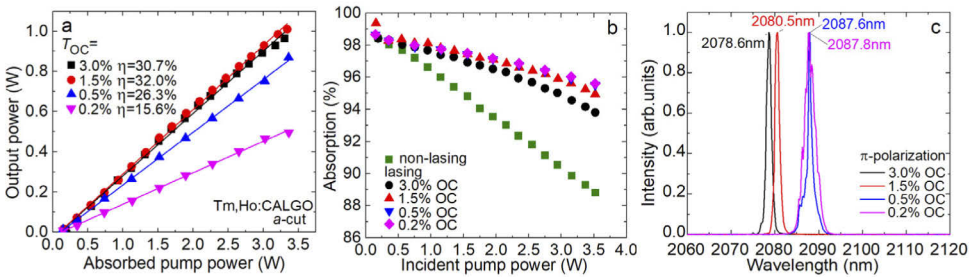


**Fig. 8.** CW laser performance of an ***a***-cut 4.5 at.% Tm, 0.5 at.% Ho:CALGO crystal: (a) input-output dependences, $\eta$ – slope efficiency, (b) measured pump absorption under lasing and non-lasing conditions; (c) typical spectra of laser emission (π-polarization).

The single-pass pump absorption under lasing conditions slightly decreased with pump power, from 98.6% to 95.0% for $T_{OC}$ = 1.5%, see Fig. 8(b). The small-signal pump absorption calculated from spectroscopic data was 98.6%. In contrast, under non-lasing conditions when the population of the upper laser level was not clamped by the threshold condition, faster decrease of the pump absorption with the pump power occurred indicating a significant bleaching of the ground-state.

Typical spectra of laser emission are shown in Fig. 8(c). The laser operated solely on the $^5I_7 \rightarrow {}^5I_8$ $Ho^{3+}$ transition, no parasitic $Tm^{3+}$ colasing was observed indicating the correctness of the selected $Ho^{3+}/Tm^{3+}$ codoping ratio. The laser emission was linearly polarized, and the polarization state (π) was naturally selected by the anisotropy of the gain, Fig. 5(c), 5(d). With increasing the output coupling, the laser wavelength experienced a blue shift, from 2087.8 nm ($T_{OC}$ = 0.2%) to 2078.6 nm ($T_{OC}$ = 3.0%). This behavior is due to the quasi-three-level scheme of the Ho laser, i.e., the inherent reabsorption influencing the emission wavelength, and it agrees with the gain spectra, Fig. 5(c).

We believe that the slope efficiency could be further improved via a careful optimization of the doping levels of $Tm^{3+}$ and $Ho^{3+}$ ions, based on both the spectroscopic characterizations and laser tests.

### 3.3. Mode-locked laser

The standard X-shaped cavity typically has two stability regions determined by the separation between the folding mirrors. The laser performance in the CW regime is optimized when aligning the laser around the center of the first stability region of the cavity corresponding to shorter $M_1$ – $M_2$ distance. We were not able to operate the laser with pure Kerr-lens mode-locking (KLM).

Optics EXPRESS

Therefore the SESAM was introduced and no hard aperture was used to support KLM. Stable ML operation could be achieved close to the second stability edge of the first region where the strength of the Kerr lens of the crystal is maximized. By continuously increasing the separation between the $M_1$ and $M_2$ mirrors towards the stability edge, self-starting CW mode-locking was achieved while the polarization state changed from π (CW regime) to σ (ML regime). Accordingly, the central laser wavelength experienced a notable blue-shift, from 2078.6 nm to 2015 nm. Druon *et al.* observed polarization-switching in Yb:CALGO crystals (from σ to π) with increasing pump power [22]. Loiko *et al.* explained this behavior by the similarity of the gain cross-sections for both polarizations and the anisotropic thermal lens [16]. The possible origin of polarization switching in our laser (from π to σ) is the additional loss introduced by the SESAM. Its high reflection band extends from 1900–2100 nm (Fig. 7(b)), i.e., the CW emission at ~2080 nm, where the π-polarization is preferred (Fig. 5(c)), is located at the long-wavelength edge of the HR range of the SESAM. With respect to the loss introduced by the SESAM and an almost zero GDD between 1900 and 2100 nm, broadband mode-locked emission centered at ~2000 nm (in our case at 2015 nm) is supported which fits with the gain cross section maximum of the σ-polarization (Fig. 5(d)). Furthermore, the broader and smoother gain profiles for σ-polarization support the generation of shorter pulses, Fig. 5(c), 5(d).

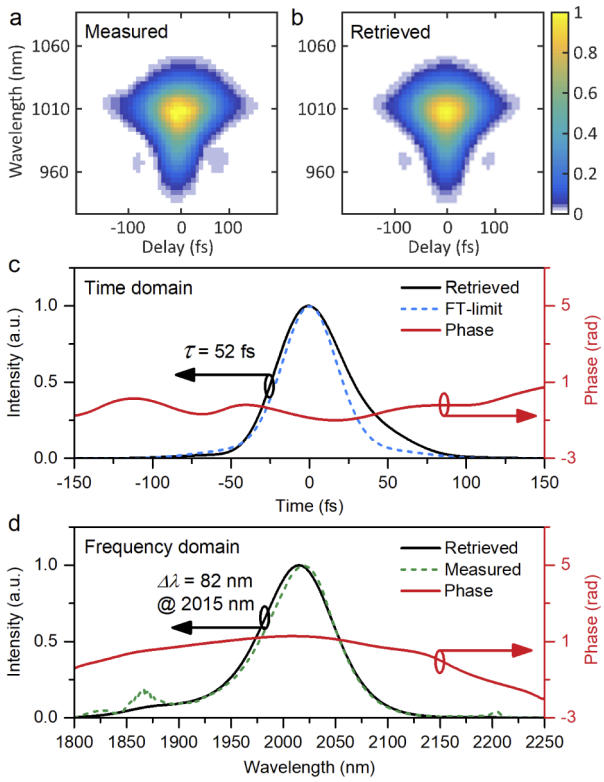


**Fig. 9.** SESAM ML Tm,Ho:CALGO laser: (a,b) SHG-FROG characterization of the shortest pulses achieved with 3.0% OC: (a) measured and (b) retrieved traces; (c) retrieved temporal profile/phase (*black/red solid curves*) and the Fourier-limited temporal profile calculated from the measured spectral profile (*blue dashed curve*); (d) retrieved spectral profile/phase (*black/red solid lines*) and the measured spectrum (*green dashed curve*). $\tau$: retrieved pulse duration (FWHM intensity), $\Delta\lambda$: spectral bandwidth (FWHM). The laser emission is σ-polarized.

Optics EXPRESS

In the ML regime of operation, at the maximum pump power, an average output power of 376 mW was achieved at a repetition rate of 86 MHz, corresponding to a pulse energy of ~4.4 nJ. The estimated fluence on the SESAM in the cavity is 300 μJ/cm$^2$. We did not observe any damage or double pulsing at this fluence level, which indicates operation well below the roll-over. The ML laser operated at a central wavelength of 2015 nm and the emission bandwidth (FWHM) was 82 nm for the 3.0% OC with which the shortest pulses were achieved. To characterize the pulse duration properly, we have used a home-made second-harmonic generation frequency-resolved optical gating (SHG-FROG) set-up. The measured and retrieved FROG traces on a 128×128 grid size are shown in Fig. 9(a) and Fig. 9(b), respectively. A total retrieval error of only 0.004 was achieved. A pulse duration (FWHM) of 52 fs was derived while from the spectral bandwidth, a Fourier-transform limited pulse duration of 45 fs was calculated.

A comparison of the measured ML spectrum with the gain spectra of the Tm,Ho:CALGO crystal, cf. Figure 5, indicates that the developed ML laser benefits from the gain originating from both $Tm^{3+}$ and $Ho^{3+}$ ions, and the combined gain bandwidth for a codoped crystal plays a key role in achieving sub-100 fs pulses. Compared to [17], the role of $Tm^{3+}$ is more pronounced in the present experiments, leading ultimately to shorter pulse durations.

The ML laser was working with superior long-term stability for hours without interrupting or power degradation. The beam profile was rather good with an $M^2$-value of about 1.3 supported by the cavity design which has almost no astigmatism because the gain crystal was operated at normal incidence and the resonator contained no other tilted elements. To characterize the stability of the ML operation, radio frequency (RF) spectra were measured with a fast extended InGaAs photodiode (EOT, ET-5000, bandwidth >10 GHz). Figure 10(a) depicts a 1 GHz wide-span RF measurement at a resolution bandwidth (RBW) of 30 kHz. The harmonic beat notes show almost constant extinction ratio with a decrease < 7 dB within the 1 GHz span. Measured in a 600 kHz span with a RBW of 300 Hz, the fundamental beat note at 85.65 MHz displays an extinction ratio of 85 dBc above carrier, Fig. 10(b), evidencing stable mode-locking without any Q-switching instabilities.

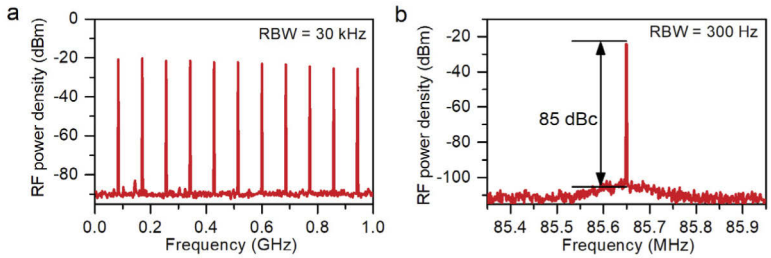


**Fig. 10.** Measured radio frequency (RF) spectra of the SESAM ML Tm,Ho:CALGO laser with 3.0% OC: (a) 1.0 GHz wide-span, (b) fundamental beat note (RBW: resolution bandwidth).

## 4. Conclusion

In conclusion, the disordered CALGO crystal codoped with $Tm^{3+}$ and $Ho^{3+}$ ions appears as a nearly ideal material for the generation of ultrashort (few-optical-cycle) pulses at 2 μm, similarly to $Yb^{3+}$-doped CALGO at 1 μm. It combines the attractive thermo-mechanical properties of the host matrix itself (i.e., high thermal conductivity with a weak concentration-dependence, weak thermal expansion and a nearly "athermal" behavior leading to weak thermal lensing), as well as advantageous spectroscopic properties of the $Tm^{3+}$ and $Ho^{3+}$ dopant ions, namely strong inhomogeneous broadening of absorption and emission bands owing to the disordered crystal structure, a notable polarization anisotropy of luminescence spectra leading to linearly

Optics EXPRESS

polarized laser output, efficient and predominantly unidirectional $Tm^{3+} \rightarrow Ho^{3+}$ energy transfer, and relatively long upper laser level lifetimes. The spectral gain profile of Tm,Ho:CALGO covers an extremely broad range from 1.85 to 2.15 µm.

In the present work, a Tm,Ho:CALGO laser passively mode-locked by a GaSb-based SESAM generated pulses as short as 52 fs at 2.015 µm featuring a broad spectral bandwidth of 82 nm. It was supported by the combined gain profiles of both the $Tm^{3+}$ and $Ho^{3+}$ ions. The main limitation for further pulse shortening is given in this work by the edges of the high reflection band of the used SESAM, as in our recent publication where a SESAM with the same reflection characteristics was applied [23]. Without such a spectral limiting SA, at present the bandwidth of the dielectric coatings of the cavity mirrors, in particular the output coupler set the limit [7]. We believe that mode-locking of other $Tm^{3+}$,$Ho^{3+}$ codoped broadband emitting materials such as mixed sesquioxides or disordered garnets could also provide extended spectral support to enable the generation of sub-50-fs pulses in the 2-µm spectral region.

**Funding.** Alexander von Humboldt-Stiftung; Région Normandie.

**Acknowledgements.** M. Guina acknowledges the support of S. Suomalainen and A. Härköneen for SESAM fabrication. Y. Zhao acknowledges financial support from the Alexander von Humboldt Foundation through a Humboldt fellowship. P. Loiko acknowledges support from the chaire d'excellence project "RELANCE" co-funded by ANR and Normandie Region (France).

**Disclosures.** The authors declare no conflicts of interest.

**Data availability.** Data underlying the results presented in this paper are not publicly available at this time but may be obtained from the authors upon reasonable request.

## References

1. T. Popmintchev, M.-C. Chen, D. Popmintchev, P. Arpin, S. Brown, S. Ališauskas, G. Andriukaitis, T. Balčiunas, O. D. Mücke, A. Pugzlys, A. Baltuška, B. Shim, S. E. Schrauth, A. Gaeta, C. Hernández-García, L. Plaja, A. Becker, A. Jaron-Becker, M. M. Murnane, and H. C. Kapteyn, "Bright coherent ultrahigh harmonics in the keV X-ray regime from mid-infrared femtosecond lasers," Science **336**(6086), 1287–1291 (2012).
2. M. Clerici, M. Peccianti, B. E. Schmidt, L. Caspani, M. Shalaby, M. Giguère, A. Lotti, A. Couairon, F. Légaré, T. Ozaki, D. Faccio, and R. Morandotti, "Wavelength scaling of terahertz generation by gas ionization," Phys. Rev. Lett. **110**(25), 253901 (2013).
3. V. Petrov, "Frequency down-conversion of solid-state laser sources to the mid-infrared spectral range using non-oxide nonlinear crystals," Prog. Quantum Electron. **42**, 1–106 (2015).
4. Y. Wang, G. Xie, X. Xu, J. Di, Z. Qin, S. Suomalainen, M. Guina, A. Härkönen, A. Agnesi, U. Griebner, X. Mateos, P. Loiko, and V. Petrov, "SESAM mode-locked Tm:CALGO laser at 2 µm," Opt. Mater. Express **6**(1), 131–136 (2016).
5. P. Loiko, J. M. Serres, X. Mateos, K. Yumashev, N. Kuleshov, V. Petrov, U. Griebner, M. Aguiló, and F. Díaz, "Microchip laser operation of Tm,Ho:$KLu(WO_4)_2$ crystal," Opt. Express **22**(23), 27976–27984 (2014).
6. Z. Pan, P. Loiko, Y. Wang, Y. Zhao, H. Yuan, K. Tang, X. Dai, H. Cai, J. M. Serres, S. Slimi, E. B. Salem, E. Dunin, A. Kornienko, L. Fomicheva, J.-L. Doualan, P. Camy, W. Chen, U. Griebner, V. Petrov, M. Aguiló, F. Díaz, R. M. Solé, and X. Mateos, "Disordered $Tm^{3+}$,$Ho^{3+}$-codoped CNGG garnet crystal: Towards efficient laser materials for ultrashort pulse generation at ~2 µm," J. Alloys Compd. **853**, 157100 (2021).
7. Y. Zhao, Y. Wang, W. Chen, Z. Pan, L. Wang, X. Dai, H. Yuan, Y. Zhang, H. Cai, J. E. Bae, S. Y. Choi, F. Rotermund, P. Loiko, J. M. Serres, X. Mateos, W. Zhou, D. Shen, U. Griebner, and V. Petrov, "67-fs pulse generation from a mode-locked Tm,Ho:CLNGG laser at 2083nm," Opt. Express **27**(3), 1922–1928 (2019).
8. Z. Pan, Y. Wang, Y. Zhao, M. Kowalczyk, J. Sotor, H. Yuan, Y. Zhang, X. Dai, H. Cai, J. E. Bae, S. Y. Choi, F. Rotermund, P. Loiko, J. M. Serres, X. Mateos, U. Griebner, and V. Petrov, "Sub-80 fs mode-locked Tm,Ho-codoped disordered garnet crystal oscillator operating at 2081nm," Opt. Lett. **43**(20), 5154–5157 (2018).
9. R. Moncorgé, N. Garnier, P. Kerbrat, C. Wyon, and C. Borel, "Spectroscopic investigation and two-micron laser performance of $Tm^{3+}$:$CaYAlO_4$ single crystals," Opt. Commun. **141**(1-2), 29–34 (1997).
10. J. A. Hutchinson, H. R. Verdun, B. H. Chai, B. Zandi, and L. D. Merkle, "Spectroscopic evaluation of $CaYAlO_4$ doped with trivalent Er, Tm, Yb and Ho for eyesafe laser applications," Opt. Mater. **3**(4), 287–306 (1994).
11. J. Di, X. Xu, C. Xia, Q. Sai, D. Zhou, Z. Lv, and J. Xu, "Growth and spectra properties of Tm, Ho doped and Tm, Ho co-doped $CaGdAlO_4$ crystals," J. Lumin. **155**, 101–107 (2014).
12. P. Loiko, P. Becker, L. Bohatý, C. Liebald, M. Peltz, S. Vernay, D. Rytz, J. M. Serres, X. Mateos, Y. Wang, X. Xu, J. Xu, A. Major, A. Baranov, U. Griebner, and V. Petrov, "Sellmeier equations, group velocity dispersion and thermo-optic dispersion formulas for $CaLnAlO_4$ (Ln = Y, Gd) laser host crystals," Opt. Lett. **42**(12), 2275–2278 (2017).
13. P. O. Petit, J. Petit, P. Goldner, and B. Viana, "Inhomogeneous broadening of optical transitions in Yb:$CaYAlO_4$," Opt. Mater. **30**(7), 1093–1097 (2008).

Optics EXPRESS


14. Y. Zaouter, J. Didierjean, F. Balembois, G. Lucas Leclin, F. Druon, P. Georges, J. Petit, P. Goldner, and B. Viana, "47-fs diode-pumped $Yb^{3+}$:$CaGdAlO_4$ laser," Opt. Lett. **31**(1), 119–121 (2006).
15. Y. Wang, X. Su, Y. Xie, F. Gao, S. Kumar, Q. Wang, C. Liu, B. Zhang, B. Zhang, and J. He, "17.8 fs broadband Kerr-lens mode-locked Yb:CALGO oscillator," Opt. Lett. **46**(8), 1892–1895 (2021).
16. P. Loiko, F. Druon, P. Georges, B. Viana, and K. Yumashev, "Thermo-optic characterization of Yb:$CaGdAlO_4$ laser crystal," Opt. Mater. Express **4**(11), 2241–2249 (2014).
17. Y. Zhao, Y. Wang, X. Zhang, X. Mateos, Z. Pan, P. Loiko, W. Zhou, X. Xu, J. Xu, D. Shen, S. Suomalainen, A. Härkönen, M. Guina, U. Griebner, and V. Petrov, "87 fs mode-locked Tm,Ho:$CaYAlO_4$ laser at ~2043 nm," Opt. Lett. **43**(4), 915–918 (2018).
18. Z. Pan, P. Loiko, J. M. Serres, E. Kifle, H. Yuan, X. Dai, H. Cai, Y. Wang, Y. Zhao, M. Aguiló, F. Díaz, U. Griebner, V. Petrov, and X. Mateos, "Mixed" Tm:Ca(Gd,Lu)AlO4 — a novel crystal for tunable and mode-locked 2 µm lasers," Opt. Express **27**(7), 9987–9995 (2019).
19. B. M. Walsh, N. P. Barnes, and B. Di Bartolo, "The temperature dependence of energy transfer between the Tm $^3F_4$ and Ho $^5I_7$ manifolds of Tm-sensitized Ho luminescence in YAG and YLF," J. Lumin. **90**(1-2), 39–48 (2000).
20. D. L. Dexter, "A theory of sensitized luminescence in solids," J. Chem. Phys. **21**(5), 836–850 (1953).
21. J. Paajaste, S. Suomalainen, A. Härkönen, U. Griebner, G. Steinmeyer, and M. Guina, "Absorption recovery dynamics in 2 µm GaSb-based SESAMs," J. Phys. D: Appl. Phys. **47**(6), 065102 (2014).
22. F. Druon, M. Olivier, A. Jaffrès, P. Loiseau, N. Aubry, J. DidierJean, F. Balembois, B. Viana, and P. Georges, "Magic mode switching in Yb:$CaGdAlO_4$ laser under high pump power," Opt. Lett. **38**(20), 4138–4141 (2013).
23. L. Wang, W. Chen, Y. Zhao, P. Loiko, X. Mateos, M. Guina, Z. Pan, M. Mero, U. Griebner, and V. Petrov, "Sub-50 fs pulse generation from a SESAM mode-locked Tm,Ho-codoped calcium aluminate laser," Opt. Lett. **46**(11), 2642–2645 (2021).